Characterization on magnetophoretic velocity of the cluster of submicron-sized composite particles applicable to magnetic separation and purification

Characterization on magnetophoretic velocity of the cluster of submicron-sized composite particles applicable to magnetic separation and purification

Natsuki KOHAMA[a], Chika SUWABE[a], Haruyuki ISHII[a], Kumiko HAYASHI[b], Daisuke NAGAO[a]

[a]Department of Chemical Engineering, Graduate School of Engineering, Tohoku University,
[b]Department of Applied Physics, Graduate School of Engineering, Tohoku University

Abstract

Submicron-sized magnetic composite particles with low polydispersity were prepared to examine the relation between the magnetophoretic velocity and the clustering state of composite particles under application of magnetic field. Five different magnetic composite particles in a size range of 70-470 nm were employed to measure the magnetophoretic velocity. Since the smallest composite particles had colloidal stability insufficient to measure the magnetophoretic velocity, the rest of composite particles was observed with an optical microscope under a magnetic field. Magnetic composite particles larger than 300 nm formed pearl chains of magnetic composite particles under the magnetic field. The velocity of pearl chains was increased by the number of composite particles nin a pearl chain. The ratio of the velocity of pearl chain to that of a single composite particle was employed to quantify the increase in magnetophoretic velocity with the clustering of composite particles. The velocity ratio for the large particles was in good agreement with the theoretical one correlated with the number of composite particles in a pearl chain. On the other hand, composite particles smaller than 200 nm formed random clusters of composite particles. Since a single small particle could not be directly observed with the optical microscope, the number of small composite particles in a cluster was estimated with an assumption that the small composite particles formed an ellipsoidal shape with a random filling factor of 0.64. Similarly to the large composite particles, the velocity ratio of random clusters composed of the small composite particles was also increased by clustering the small MCPs. Comparison of the velocity ratios between different composite particles indicated that the clusters of small particles have a tendency of exhibiting velocity ratios higher than that of large particles. A good correlation of the velocity ratio with the estimated number of composite particles in a cluster revealed that the number of composite particles is an important factor to quantify the magnetophoretic velocity of random clusters.

Keywords :   Magnetic composite particles; Magnetophoresis; Monodispersity

1.   Introduction

Magnetic nanoparticles (NPs) such as Fe_3O_4 and γ-Fe_2O_3 NPs have a variety of promising applications including therapeutic applications such as magnetic separation and purification [1–4], drug delivery [5] and hyperthermia [6,7]. They can also be employed as reusable carriers in biomolecule separation [8] and enzyme reaction [9,10] because of their responsivity to an external magnetic field [11]. Recently, the use of magnetic NPs as carriers have been applied to biosensors, microfluidics and lab-on-a chip [12,13].

The responsivity of the magnetic NPs has to be maintained in air or in dispersion media such as water which oxidizes the NPs to deteriorate their magnetic properties [14]. In addition to the high responsivity to a magnetic field, NPs provided with scaffold to support enzymes and linkers are required in the application of carriers for biomolecules. Aggregation of NPs should be avoided because it lowers specific surface areas of the NPs. Coating of NPs or NP assemblies with outer shell is commonly used to enhance their colloidal stability in water and also to provide NPs with scaffolds [15–18].

Another problem in the application of NPs to magnetic separation and purification is their low magnetic moment in an isolated state, making it difficult to be magnetically transported due to their thermal fluctuation stronger than magnetophoretic forces [19]. NPs clustering induced by a magnetic field is a practical approach to overcome the low responsivity of NPs because the magnetic moments of NPs in a cluster can be cooperatively oriented under the magnetic field [20].

To obtain magnetic composite particles (MCPs) with a high responsivity to magnetic field, our group developed a collective approach in which magnetic NPs are electrostatically heterocoagulated onto monodisperse polymer cores and followed by the silica coating [21,22]. The former process of heterocoagulation was able to enhance the magnetic responsivity of composite particles, and the

latter of silica-coating to form a protective layer against the oxidation was able to provide the heterocoagulated particles with a scaffold layer for biomolecules. Our approach is useful for the preparation of submicron-sized MCPs and has a distinct advantage in particle monodispersity over other synthetic methods previously reports [10,11].

The magnetic responsivities of magnetic NPs and MCPs have been evaluated by measurements of saturation magnetization or the time for particles to be collected under a magnetic field [9,20,23,24]. Since magnetic NPs and MCPs tend to form clusters under the magnetic field [19,25], the clustering state of particles in dispersion media should be understood for precisely controlling the NP transportation under the magnetic field.

Wise et al. employed an optical microscope to directly measure magnetophoretic velocity of magnetic particles dispersed in water [26]. They observed pearl-chain structure of the magnetic particles and compared the velocity of the chain-structured particles with that of a single magnetic particle. They characterized megnetophoretic velocities of micron-sized particles that were readily observed with an optical microscope. Submicron-sized, magnetic particles applicable to carriers in lab-on-chip and enzyme reactions, however, have not been characterized so far to understand the clustering state of particles under a magnetic field. A reason not to be able to quantify the magnetophoretic velocity of submicron-sized MCPs was low monodispersity of the submicron-sized MCPs previously prepared.

In the present work, highly monodisperse, submicron-sized magnetic particles prepared by our previous method are employed to clarify the correlation of their magnetophoretic velocity with clustering states of NPs. Monodisperse magnetic particles with different sizes in a range of 100–500 nm were characterized to examine particle sizes suitable as carriers for biomaterials [9,10,12,13]. A well-designed carrier with a high specific surface area and a high responsivity is allowed to improve the efficiency of magnetic recovery. In the application of lab-on-chip for diagnostic screening tests which uses the difference in magnetophoretic velocity between clustered particles [12], the high-throughput detection of disease is expected in the well-designed carriers.

2.   Materials and methods

2.1.   Materials

3-Methacryloxypropyltrimethoxysilane (MPTMS, 95%) was obtained from JNC Corporation (Tokyo, Japan). Ammonia solution (25%), iron(III) chloride ($FeCl_3$, 95%), tetraethylorthosilicate (TEOS, 95%), ethanol (99.5%), methylmethacrylate (MMA, 98.0%), styrene monomer (St, 99.0%), sodium p-styrenesulfonate (NaSS, 80%), potassium persulfate (KPS, 95.0%), ammonium persulfate (APS, 98%) and sodium dodecyl sulfate (SDS) were purchased from Wako Pure Chemical Industries (Osaka, Japan). Iron(II) chloride ($FeCl_2$, 99.9%, Superpurification Science Laboratory, Saitama, Japan), N-trimethoxysilylpropyl-N,N,N-trimethylammoniumchloride (TSA, 50%methanol solu tion) were purchased from Gelest Ink. (U.S.). 3-Methacryloxypropylmethyldimethoxysilane (MPDMS, 98.0%) was obtained from Shinetsu Chemical (Tokyo, Japan). The inhibitor for monomers of MMA and St was removed by an inhibitor removal column. Water was deionized (>18.2MΩ cm). The other chemicals were used as received.

2.2.   Preparation of positively charged magnetite nanoparticles

Magnetite nanoparticles were prepared by a modified Massart method [24,27]. The magnetic nanoparticles prepared in the coprecipitation of $FeCl_3$ and $FeCl_2$ were cationized by surface-modification of the nanoparticles with quaternary-amine coupling agent (TSA) in the Massart method. TSA was added into the nanoparticles suspension 30 s after the initiation of the coprecipitation.

2.3.   Preparation of negatively charged polymer particles

Monodisperse polymer particles with average sizes ranging from 50 to 470 nm were prepared in emulsion polymerization or soap-free emulsion polymerization.

For the particles with an average size of 50 nm(P1), emulsion polymerization was employed according to our method previously reported [28]. In the polymerization MMA and St were copolymerized at the concentrations of 0.15M and 0.15 M, respectively. The SDS aqueous solution was bubbled with N_2 gas under stirring for 30 min. Then, monomers of St and MMA were added to the aqueous solution, which was stirred for 20 min under N_2 atmosphere. To initiate polymerization, 30 ml of aqueous APS solution was added into the reactor. The polymerization was performed for 6 h under nitrogen atmosphere at 70 °C.

For the particles with average sizes from 100 to 200 nm, soap-free emulsion polymerization was employed. In the polymerization, MMA and NaSS were used as a main monomer and an anionic comonomer, respectively. The polymerization of the monomers was initiated with KPS at 65 °C under stirring in water that was deoxygenated by bubbling with nitrogen for 30 min before use. The NaSS and KPS are anionized in water to have opposite charges against the surface of the magnetite nanoparticles with TSA-modified [21].

Forty minutes after the initiation of the polymerization a silane coupling agent of MPTMS was added to the reactant solution [22]. The polymerization was performed for 2 h under nitrogen atmosphere. The concentrations of MMA, NaSS, KPS and MPTMS were 0.20 M, 1.0 mM, 6.4mM and 4mM for 100 nm polymer particles (P2). The concentrations of agents for 200 nm particles (P3) are summarized in Table S1.

For the particles with average sizes from 300-500 nm, St was used as a main monomer. The polymerization of St was initiated at 70 °C under stirring with KPS in water that was deoxygenated by bubbling with nitrogen for 30 min before use. Another silane coupling agent of MPDMS was added to the reactant solution 2 h after the initiation of the polymerization. The polymerization was performed for 6 h under nitrogen atmosphere. The concentrations of St, KPS and MPDMS were 0.115 M, 5.0 mM, and 10mM for 300 nm polymer particles (P4). The concentrations of agents for 500 nm particles (P5) are summarized in Table S1.

2.4. Preparation of magnetic composite particles

Magnetic composite particles (C1–C5) were prepared by the combined process of heterocoagulation and silica-coating according to our method previously reported [21]. A mixed suspension of the magnetic NPs and the polymer particles was shaken for a minute after the mixing. The concentrations of magnetic NPs and polymer particles in the heterocoagulation are listed in Table S2. The nanoparticles that were not adsorbed onto the polymer particles were removed in a combined washing process of centrifugation and redispersion. To the suspension of heterocoagulates (H1–H5) that were sonicated for 1.5 h, an ethanolic solution of water, ammonia, TEOS and MPTMS was successively added at ambient temperature to initiate the hydrolysis and condensation of silicon alkoxides [29]. The suspension mixed with the silica sources was shaken 24 h. The suspension obtained by the Stöber reaction was washed in the above combined process for the characterization. The concentrations of the heterocoagulates, TEOS, MPTMS, water and ammonia were 0.12 vol%, 5 mM, 5 mM, 9 M, 0.3M for 100 nm particles, respectively. The silica-coating concentrations for the other heterocoagulates were listed in Table S3.

2.5. Observation of MCPs by optical microscope

MCPs suspension was observed at room temperature with an optical microscope (IX 71, Olympus, Tokyo, Japan) under a magnetic field. MCP suspension at a particle concentration of 1×10^{-4} vol% was put into a gap space between two glass plates with different dimensions (32mm×24mm and 16mm×16 mm, Matsunami Glass Ind, Ltd, Tokyo, Japan) with a spacer of paraffin film. The two glass slides were coated with a solution of BSA (0.5 wt%, Wako Pure Chemical Industries, Osaka, Japan). The MCPs in the gap space were observed with the optical microscope. The microscopic observation was performed using 100× objective lens (UPlanSApo 100×/1.40, Olympus) and sCMOS camera (OLCA-Flash4.0 V2, Hamamatsu Photonics, Hamamatsu, Japan). The magnetic field was applied to the suspension of MCPs using electromagnet (Toei Scientific Industrial Co., Sendai, Japan). DC power was supplied by compact DC power supply (DC80-27, NF Corporation, Yokohama, Japan). The strength of magnetic field was adjusted to 0.3 T.

2.6. Characterization

The synthesized particles were observed with FE-TEM (Hitachi, HD-2700). Colloidal stabilities of the particles were monitored using dynamic light scattering (DLS, Otsuka Electronics, ELS-Z). Saturation magnetization of each particles was measured by a vibrating sample magnetometer (VSM, Toei Scientific Industrial Co.).

3. Results and discussion

Magnetic composite particles (MCPs) with average sizes ranging from 70 nm to 470 nm were prepared by our method [21] to examine the correlation between clustering states of the MCPs and their magnetophoretic velocities. Fig. 1(a)–(e) shows TEM images of the MCPs prepared in the method, which were finally obtained under the conditions of C1-C5 in Table S3. Almost all polymer particles used as cores were found to be covered with magnetic NPs, although a small amount of particles non-adsorbed onto polymer particles were observed in the TEM images. The smallest MCPs with an average size of 73 nm, however, could not sufficiently dispersed in water under no application of magnetic field (See the DLS results in Fig. S1(a) of supporting information). The other MCPs in the range of 110 to 470 nm were confirmed to be stable in water (again see Fig. S1). Coefficients of variation (C_V) of the MCP sizes, which are listed in Table S4 of supporting information, indicated that the MCPs had monodispersity high enough to be employed as model carriers for examining the dependence of magnetic responsivity on the particle size.

The saturation magnetizations (M_S) of the MCPs are plotted against the particle size in Fig. 2. The dashed line in the figure shows

the theoretical M_S values calculated on an assumption that polymer particles are covered with a monolayer of close-packed magnetic NPs using a saturation magnetization of NPs (=60 emu/g), NP density (=5.17 g/cm^3), PMMA density (=1.2 g/cm^3) and polystyrene density (=1.04 g/cm^3). Both experimental and calculated M_S values in the figure were increased with a decrease in particle size due to the high surface-to-volume ratio in small polymer particles. A good correlation of the experimental M_S with the calculated one suggests full-monolayer coverage of the polymer particles with the magnetic NPs.

Behaviors of the MCPs in an aqueous suspension (1×10^{-4} vol%) were observed with an optical microscope. Microscope images of the clustered MCPs observed less than 15 s and more than 30 s after the initiation of field application are presented in the upper and lower rows of Fig. 3, respectively. Interactions that should be considered for MCPs in suspensions under application of magnetic field are van der Waals interaction, electrostatic interaction, and magnetic dipole-dipole interaction [30]. The MCPs smaller than 200 nm in Fig. 3 exhibited a tendency of being randomly clustered just after the initiation, forming rod-shaped assemblies. The application of magnetic field elongated the random clusters of MSPs to the field direction.
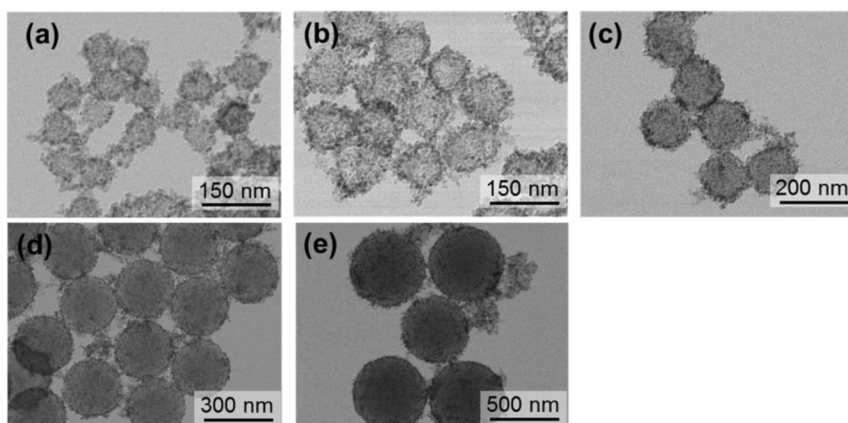

Fig. 1. TEM images of magnetic composite particles prepared under different conditions summarized in Table S1–S3.
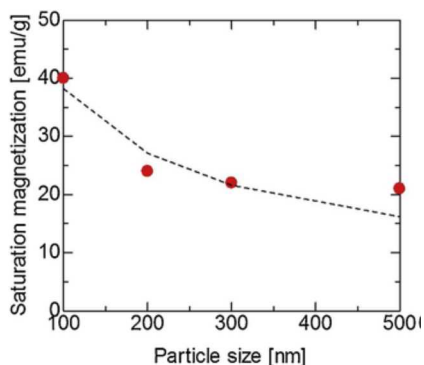

Fig. 2. Dependence of saturation magnetization on sizes of magnetic composite particles. The dashed line shows the theoretical M_S values based on an assumption of monolayer coverage of close-packed magnetic NPs on polymer particles In the calculation of M_S values, the saturation magnetization of magnetic NPs (=60 emu/g), NP density (=5.17 g/cm [33], PMMA densities (=1.2 g/cm3)and polystyrene density (=1.04 g/cm [3]) were used.

The diffusion of small particles in suspension is generally stronger than that of large particles, suggesting that small particles tend to isotropically collide with each other overcoming electrostatic repulsion between the particles in water. According to previous reports [30,31], in which the ratio (λ) of the interparticle interaction of mdd to the thermal energy was used as a parameter to discuss the cluster morphology of particles, random clusters of particles were formed under a magnetic field with λ lower than 3. On the other hand, it was reported for high λ values that pearl chain structures of particles were formed under the field application. Fig. 3 experimentally indicated that the MCPs larger than 300 nm formed a pearl chain structure without random agglomeration and extended their chain length during the application of magnetic field at λ -3.3.

Magnetophoretic velocities of the MCPs were measured under the magnetic field with ~0.3 T. The velocities of clusters more than 30 s after the initiation of field application were plotted against the cluster length of 500 nm MCPs in Fig. 4. Longer clusters exhibited

higher velocity under the magnetic field, indicating that the formation of clusters facilitated the magnetophoresis of MCPs. Wise et al. proposed the ratio between the velocity of particle cluster and that of a single particle to quantify the transportation of particle clusters [26]. According to their report, the megnetophoretic velocity ratio for 500 nm particles are presented in Fig. S2 where the number of MCPs in a cluster was calculated from the measured length divided by the average size of MCPs. The velocity ratio was found to be increased almost three times by the clustering of MCPs under the magnetic field.

Velocity ratios of clusters for the other MCPs with different averages sizes are presented in Fig. S3 (a)–(c), respectively. The number of MCPs in a cluster for 100 nm and 200 nm particles, which formed rod-shaped random clusters, were calculated with an ellipsoidal approximation for each rod-shaped cluster. The estimation of the average number of MCPs in a cluster is described in details in Supporting Information. A possible way to identify each small MCP in a cluster is a combination of fluorescently labelled MCP and fluorescence microscope, which still needs other approximations to estimate the number of MCPs three-dimensionally clustered.

The magnetophoretic velocity for a single MCP for small particles (110 nm or 170 nm) (v_s) was calculated with the following Eq. (1) [26].

$$v_s = \frac{\Delta_x V |\Delta B^2|}{12\pi\eta r \mu_0}$$ (1)

Where μ_0 is space permeability, χ is susceptibility, V is particle volume, B is magnetic flux density, η is viscosity, r is diameter. The four series of velocity ratios were compared in Fig. 5 together with theoretical velocity ratio drawn with the solid line. The theoretical ratios were estimated with Eq. [3] that is derived from a combination of Eqs. (1) and (2) [26].

$$v = \frac{\Delta_x V |\Delta B^2|}{8\pi\eta r \mu_0} \cdot \frac{\left(\frac{2n^2-1}{(n^2-1)^{\frac{1}{2}}}\right)\ln\left[n+(n^2-1)^{\frac{1}{2}}\right]-n}{n^2-1}$$ (2)
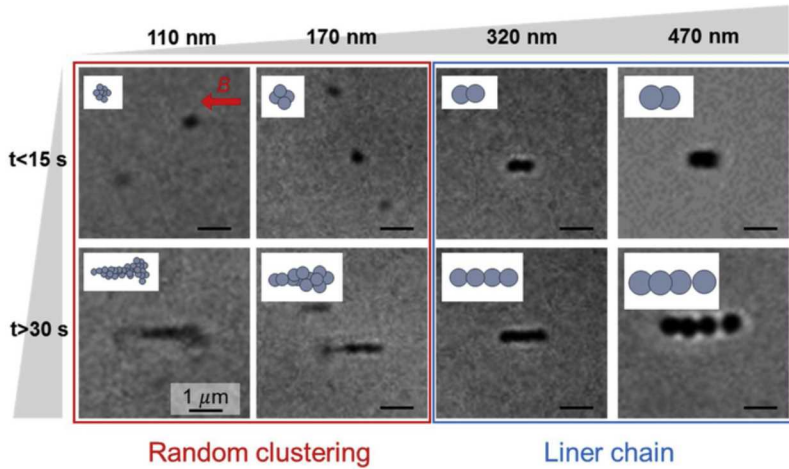

Fig. 3. Optical microscope images of magnetic composite particles with four different sizes under a magnetic field of 0.3 T. The images in the upper and lower rows were taken less than 15 s and more than 30 s after initiation of the field application, respectively.
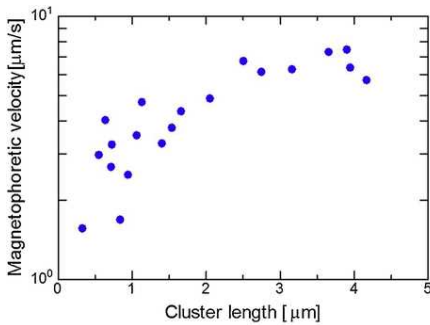

Fig. 4. Magnetophoretic velocity of the cluster of magnetic composite particles with an average size of 470 nm. The cluster length was experimentally estimated in the optical microscope image.
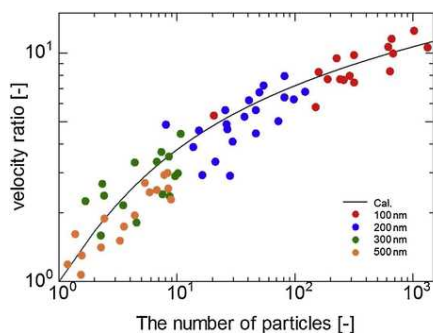
Fig. 5. The ratio of the magnetophoretic velocity of clusters to that of a single particle for MCPs with different sizes in a range of 110 nm—470 nm. The filled circles and solid line show the experimental and theoretical ratio, respectively. The velocity ratio in the number range up to 100 is shown in Fig. S3 to compare the velocity ratio for large MCPs.

where n is the number of particles.

$$\frac{v}{v_s} = \frac{3}{4} \frac{\left(\frac{2n^2-1}{(n^2-1)^{\frac{1}{2}}}\right)\ln\left[n+(n^2-1)^{\frac{1}{2}}\right]-n}{n^2-1} \tag{3}$$

The velocity ratios for different sizes of MCPs in Fig. 5 were correlated well with the theoretical line of Eq. (3).

Interestingly, magnetophoretic velocity ratios higher than 5 were observed for the rod-shaped clusters of MCPs smaller than 200 nm, whereas they could not be attained in the pearl chain clusters of MCPs larger than 300 nm.

At a constant amount of MCPs dispersed in water (1×10^{-4} vol%) and an average aspect ratio (1.2) of rod-shape clusters, total surface area of clusters of small MCPs is generally higher than that of large MCPs as shown in Fig. S4. High total surface areas of MCP clusters are advantageous to support enzymes and linkers on the MCP surfaces. As shown in the size distribution of Fig. S1, however, excessive down-sizing of MCPs lowers their surface area usable for supporting enzymes and linkers due to the low colloidal stability of MCPs in the system. Considering both the high responsivity of rod-shaped cluster of small MCPs and the dependence of total surface area on the MCP size, MCPs with sub-micrometer sizes should be appropriately clustered to attain high-throughput separation or recovering systems under application of magnetic fields.

4. Conclusion

The dependence of the magnetophoretic velocity of MCPs on the clustering state was examined with monodisperse MCPs with different sizes in a range of 110-470 nm. Pearl chains and rod-shaped random clusters were observed for the MCPs larger than 300 nm and smaller than 200 nm, respectively. The threshold of particle size to distinguish the two different states of clustering is reported at the first time in the present work using the monodisperse MCPs. For both structures of MCPs, magnetophoretic velocities were correlated well with the number of MCP in a pearl chain or a random cluster. The velocity ratio of random cluster to a single small MCP was apparently higher than that of pearl chain to a single large MCP. Considering both the magnetophoretic velocity and the total surface area of clusters usable for supporting molecules, small MCPs with a high magnetoresponsivity and a high colloidal stability under no magnetic field can be practical carriers in efficient separation and purification systems using external magnetic field.

Appendix A. Supplementary data

Supplementary material related to this article can be found, in the online version, at doi:https://doi.org/10.1016/j.colsurfa.2019.02.011.

References

[1] T.H. Min, H.J. Choi, N.H. Kim, K. Park, C.Y. You, Colloids Surf. A Physicochem. Eng. Asp. 531 (2017) 48–55.

[2] G.B. Khomutov, V.P. Kim, Y.A. Koksharov, K.V. Potapenkov, A.A. Parshintsev, E.S. Soldatov, N.N. Usmanov, A.M. Saletsky, A.V. Sybachin, A.A. Yaroslavov, I.V. Taranov, V.A. Cherepenin, Y.V. Gulyaev, Colloids Surf. A Physicochem. Eng. Asp. 532 (2017) 26–35.

[3] L.M. Sanchez, D.A. Martin, V.A. Alvarez, J.S. Gonzalez, Colloids Surf. A Physicochem. Eng. Asp. 543 (2018) 28–37.

[4] W. Wang, H. Zhang, J. Shen, M. Ye, Colloids Surf. A Physicochem. Eng. Asp. 553 (2018) 672–680.

[5] T.K. Jain, M.A. Morales, S.K. Sahoo, D.L. Leslie-Pelecky, V. Labhasetwar, Mol. Pharm. 2 (2005) 194–205.

[6] K. Hayashi, M. Nakamura, W. Sakamoto, T. Yogo, H. Miki, S. Ozaki, M. Abe, T. Matsumoto, K. Ishimura, Theranostics 3 (2013) 366–376.

[7] W. Wang, B. Tang, B. Ju, S. Zhang, RSC Adv. 5 (2015) 75292–75299.

[8] L. Zhang, S. Qiao, Y. Jin, H. Yang, S. Budihartono, F. Stahr, Z. Yan, X. Wang, Z. Hao, G.Q. Lu, Adv. Funct. Mater. 18 (2008) 3203–3212.

[9] W. Wang, Y. Xu, D.I.C. Wang, Z. Li, J. Am. Chem. Soc. 131 (2009) 12892–12893.

[10] A.M. Vaz, D. Serrano-Ruiz, M. Laurenti, P. Alonso-Cristobal, E. Lopez-Cabarcos, J. Rubio-Retama, Colloids Surf. B Biointerfaces 114 (2014) 11–19.

[11] J. Cui, Y. Feng, S. Yue, Y. Zhao, L. Li, R. Liu, T. Lin, J. Chem. Technol. Biotechnol. 91 (2016) 1905–1913.

[12] W. Huang, C.-L. Chang, N.D. Brault, O. Gur, Z. Wang, S.I. Jalal, P.S. Low, T.L. Ratliff, R. Pili, C.A. Savran, Lab Chip 17 (2017) 415–428.

[13] A. van Reenen, A.M. de Jong, M.W.J. Prins, Anal. Chem. (2019) https://doi.org/10.1021/acs.analchem.6b04043, in press.

[14] A.H. Lu, E.L. Salabas, F. Schüth, Angew. Chemie - Int. Ed. 46 (2007) 1222–1244.

[15] V.I. Shubayev, T.R. Pisanic, S. Jin, Magnetic nanoparticles for theragnostics, Adv. Drug Deliv. Rev. 61 (2009) 467–477.

[16] C. Wang, J. Yan, X. Cui, H. Wang, J. Colloid Interface Sci. 354 (2011) 94–99.

[17] X. Mu, J. Qiao, L. Qi, P. Dong, H. Ma, ACS Appl. Mater. Interfaces 6 (2014) 21346–21354.

[18] J. Park, M.D. Porter, M.C. Granger, ACS Appl. Mater. Interfaces 9 (2017) 19569–19577.

[19] G. De Las Cuevas, J. Faraudo, J. Camacho, J. Phys. Chem. C 112 (2008) 945–950.

[20] T. Leshuk, H. Krishnakumar, F. Gu, J. Nanosci. Nanotechnol. 15 (2015) 5378–5383.

[21] C. Suwabe, N. Yamauchi, D. Nagao, H. Ishii, M. Konno, Colloid Polym. Sci. 294 (2016) 2079–2085.

[22] C. Suwabe, D. Nagao, H. Ishii, M. Konno, Colloid Polym. Sci. 293 (2015) 2095–2100.

[23] S. Xu, F. Yang, X. Zhou, Y. Zhuang, B. Liu, Y. Mu, X. Wang, H. Shen, G. Zhi, D. Wu, ACS Appl. Mater. Interfaces 7 (2015) 20460–20468.

[24] H. Matsumoto, D. Nagao, M. Konno, Langmuir 26 (2010) 4207–4211.

[25] A. Okada, D. Nagao, T. Ueno, H. Ishii, M. Konno, Langmuir 29 (2013) 9004–9009.

[26] N. Wise, T. Grob, K. Morten, I. Thompson, S. Sheard, J. Magn. Magn. Mater. 384 (2015) 328–334.

[27] R. Massart, IEEE Trans. Magn. 17 (1981) 1247–1248.

[28] H. Ishii, N. Kuwasaki, D. Nagao, M. Konno, Polymer (Guildf) 77 (2015) 64–69.

[29] W. Stober, A. Fink, D. Ernst Bohn, J. Colloid Interface Sci. 26 (1968) 62–69.

[30] V. Tan Tran, H. Zhou, S. Lee, S. Cheol Hong, J. Kim, S.-Y. Jeong, J. Lee, ACS Appl. Mater. Interfaces 7 (2015) 8650–8658.

[31] Y. Lalatonne, J. Richardi, M.P. Pileni, Nat. Mater. 3 (2004) 121–125.